EXPERIMENTAL STUDY OF DAMAGE KINETICS IN α/β TITANIUM ALLOYS

A.L. HELBERT, X. FEAUGAS, M. CLAVEL
Université de Technologie de Compiègne, Division Mécanique
Laboratoire LG2mS, URA CNRS 1505
BP 649 60206 Compiègne Cédex, France

ABSTRACT

Nucleation and growth kinetics in α/β titanium alloys have been experimentally and numerically investigated. Efforts were focused on the triaxiality effect. Experiments were performed on different types of specimens in order to use the local approach to fracture. It has been evidenced that internal stresses increase both nucleation and growth kinetics. Void growth has been divided into two stages. The first occurs in the α-grains and the second through the surrounded β-matrix. In the second stage, growth rate strongly depends on the λ/ϕ ratio (where λ is the center-to-center particle spacing and ϕ the particle diameter).

KEYWORDS

Void nucleation and growth kinetics, α/β titanium alloys, triaxiality, internal stresses, local approach to fracture, Gurson-Tvergaard's model.

INTRODUCTION

Void nucleation and growth kinetics have been largely studied for alloys containing hard inclusions (Argon and Im, 1975; Le Roy *et al.*, 1981; Beremin, 1981; Brownrigg *et al.*, 1983; Marini *et al.*, 1985 ; Becker *et al.*, 1987; Gilormini *et al.*, 1988;...). These authors have revealed the influence of mechanical parameters such as the hardening rate, $d\sigma/d\varepsilon_{peq}$, or the triaxiality, $\chi=\sigma_m/\sigma_{eq}$, on the damage development, but also the role of the morphological parameters like the initial volume fraction of porosity or the λ/ϕ ratio (where λ is the center-to-center particle spacing and ϕ the particle diameter). Only few studies have focused on damage kinetics for materials containing soft inclusions such as α-particles in α/β titanium alloys. A few results (Margolin *et al.*, 1980) report the effects of morphological parameters on the damage kinetics under low triaxiality, however the effect of triaxiality remains poorly studied. The purpose of this work is to focus on void nucleation and growth kinetics in α/β titanium alloys and to specify the influence of mechanical and microstructural parameters on these kinetics under a wide range of triaxialities.

EXPERIMENTAL PROCEDURE

Materials:

Three α/β titanium alloys were studied: the 6246 (773 K) alloy and the TA6V (300 K) alloy which presents two different microstructures (TA6Vg and TA6Va) resulting from various heat treatments. Chemical compositions and heat treatments for each alloy are given elsewhere (Helbert *et al.*, 1996a, b). In particular, all the materials studied have the same content of aluminum (5% wt). The microstructure of these alloys is composed of a primary α-phase (h.c.p. soft phase) surrounded by a β-phase (b.c.c. hard phase). The β–phase can be transformed (in 6246, TA6Vg) and is then composed of a mixture of residual β-phase and secondary α-phase. The main mechanical and microstructural parameters are reported in table 1. The h.c.p texture is

Table 1: Mechanical and microstructural parameters of the three α/β titanium alloys. The hardening law has been chosen: $\sigma=\sigma_0 + K(\varepsilon p)^n$ where σ_0 is the yield stress. λ is the mean center-to-center α-particle spacing.

Alloys	E (GPa)	σo(2E-4)	σmax (MPa)	εl	εd	n	K (MPa)	%α	%β	φα (μm)	λ (μm)	λ/φ
TA6Va	110.0	900.0	1120.2	0.134	-0.23	0.3	479.5	50	50	5.0	5.2	1.02
TA6Vg	130.2	912.2	1072.6	0.165	-0.25	0.43	453.4	47	52	15.0	34.1	2.30
6246	109.6	740.8	1004.0	0.10	-0.38	0.75	7646	33	67	5.7	14.8	3.08

similar for all the alloys studied and was previously described (Helbert *et al.*, 1996a, b). An important number of heterogeneity levels are generally observed in α/β titanium alloys (prior-β grains, two phases (α_p and β), transformed β structure, α_2 (Ti_3Al) precipitation in the α-phase, ...) (Margolin *et al.*, 1980; Helbert *et al.*, 1996a; Feaugas *et al.*, 1995). Plastic strain incompatibilities which result from these microstructural heterogeneities, induce important internal stresses. This explains the high value of the back stress (X) generally observed in α/β titanium alloys (Feaugas *et al.*, 1995). This particular component of the macroscopic stress is obtained using the Cottrell's method (1953). This method has been previously applied for the three materials studied here (Helbert *et al.*, 1996c) and the results are given in table 2.

Table 2: Saturated values of the macroscopic stress σ, the effective stress σ_{ef} and the back stress X.

Alloys	σs (MPa)	σefs (MPa)	Xs (MPa)
TA6Va	1124	450.0	674.0
TA6Vg	1110	467.0	643.0
6246	1004	391.2	612.8

Experiments and Calculations:

The local approach of fracture has been used for the void nucleation study of the three α/β titanium alloys. This method was largely described on steels and aluminum (Beremin, 1981; Hancock and Brown, 1983; Walsh *et al.*, 1989) and allows to examine a wide range of triaxialities with the use of axisymetric notched specimens labeled AE2, AE4 and AE10. As far as the damage is studied under high and low triaxiality, smooth specimens (TL) were also used. The specimens were tested to fracture or interrupted before fracture. Besides, a finite element calculation was performed for each specimen design to provide the mechanical parameters distribution in the bulk of the specimen during loading. The mesh is reorganized so as to take into account displacement. For each material, an elasto-plastic law is identified, from the plastic behavior of the alloy before necking, in the framework of the classical elasto-plastic theory (Chaboche, 1989). It has been experimentally demonstrated that it was not necessary to take into account damage in the behavior law since, just before fracture, the hydrostatic part of strain ε_{kk} remains lower than 0.0025 (Helbert, 1996c). The validity of such calculations was checked comparing the experimental and calculated loading curves (Fig. 1) of notched specimens. The identification of the plastic law as described above allows the determination, during necking, of accurate calculated loading curves for smooth specimens (TL) (Fig. 2). Figure 2 shows the good agreement between calculated and experimental displacements during loading up to fracture. This macroscopic validity can be completed by a microscopic analysis of the local plastic strain of the α-particles measured from their shape (Helbert *et al.*, 1996a; Bourgeois *et al.*, 1996). If this local plastic strain is close to the calculated one, calculations are satisfactory.

Metallography and damage observations:

To understand the damage development, midsections of the specimens were polished and etched to be examined in the SEM. The midsection is divided into surface elements of 0.025 mm², in which the number of voids, N_a, as well as their length, L, are measured. Each of these elements are characterized by mechanical parameters provided by calculations (Helbert *et al.*., 1996a).

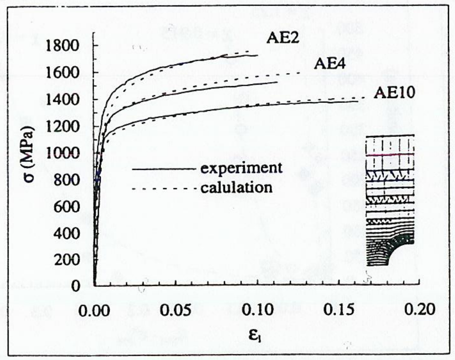

Fig. 1: Experimental and calculated loading curves (σ *vs* ε_l) for notched specimens (TA6Va).

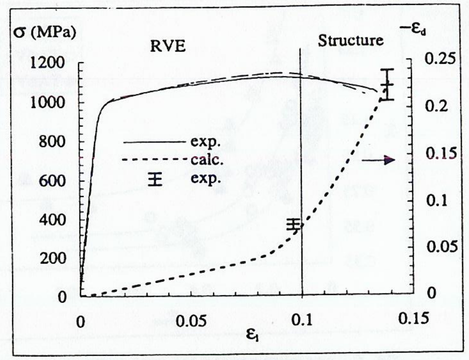

Fig. 2: Experimental and calculated loading curves (σ *vs* ε_l) for the smooth specimen (TA6Va). ε_l and ε_d are the longitudinal and the diametral strains.

RESULTS AND DISCUSSION

Void nucleation:

Previous works on the α/β titanium alloys studied here have evidenced the nature of voids created in such materials, their physical origins and the associated nucleation criterion (Margolin *et al.*, 1980; Helbert *et al.*, 1996a, b, c). Voids form at the α/β interfaces or in the α-grains. The former voids are observed for the three materials whereas voids in α-grains are only present in the TA6Vg alloy. Observations and calculations allowed to conclude that both plastic strain and hydrostatic stress are necessary to create cavities (Fig. 3). A void nucleation criterion at the α/β interface, based on these two parameters, was identified for each material (table 3 and eq.1).

$$\varepsilon^{a}_{peq} = -A\ \ln(B\chi - C) \tag{1}$$

The plastic strain needed for nucleation, ε^{a}_{peq}, is a function of triaxiality for α/β voids and ε^{a}_{peq} is constant and equals 0.05 for α-grain voids. In fact, it has been shown that the plastic strain needed for nucleation depends on the back stress X and its rate $dX/d\varepsilon_{peq}$ (the kinematic hardening rate) under a given hydrostatic stress (Helbert *et al.*, 1996c). The purpose of the present work is not to detail the nucleation criterion part since it is done elsewhere (Helbert *et al.*, 1996c), but more to focus on void nucleation and growth kinetics.

Table 3: α/β voids nucleation criteria for the three alloys studied.

	A	B	C
TA6Va	0.128	1	0.5
TA6Vg-α/β	0.133	0.66	0.35
6246	0.143	0.45	0.31

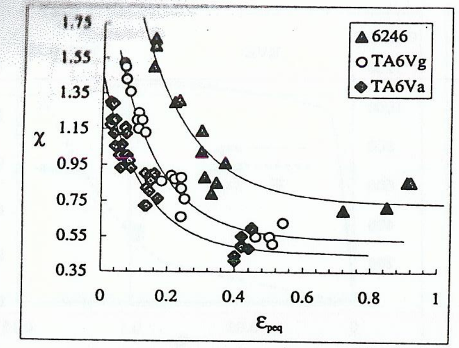

Fig. 3: Triaxiality needed for void nucleation at the α/β interface *vs* plastic strain.

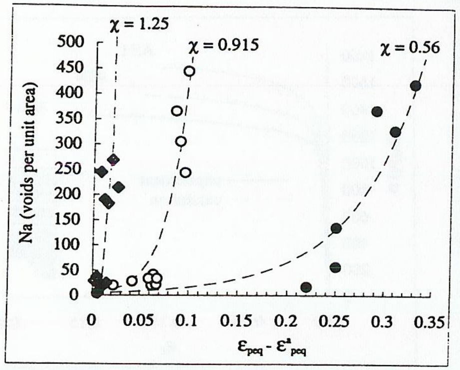

Fig. 4: Void density *vs* (ε_{peq}- ε^{a}_{peq}) for different stress triaxialities and their associated calculated curves with eq.3 (TA6Va).

Void nucleation kinetics:

Using all specimens strained, it is possible to plot the number of voids per unit area, N_a, *vs* plastic strain for different triaxialities. This plot reveals an exponential increase (Fig. 4) whatever the alloy. Both non-linear plot of N_a *vs* ε_{peq} and dependence of this plot on triaxiality have already been observed on iron-based materials (Brownrigg *et al.*, 1983) and aluminum alloys (Walsh *et al.*, 1989). The exponential increase has also been reported on spheroidized steels (Le Roy *et al.*, 1983) and Ti-5-5 alloys (Greenfield *et al.*, 1972). As previously shown (Chu *et al.*, 1980), the rate of voids nucleated per unit area dN_a/N_a can be expressed as:

$$dN_a/N_a = D\, d\varepsilon_{peq} \qquad (2)$$

where D is a function of triaxiality. In α/β titanium alloys, D=E exp (Fχ) seems to be well adapted to describe the experimental results (Fig. 4). So as to account for the change in N_a with (ε_{peq}- ε^{a}_{peq}) (Fig. 4), the following relationship is obtained:

$$N_a = N_o \exp\left[D(\varepsilon_{peq} - \varepsilon^{a}_{peq})\right] \qquad (3)$$

N_o corresponds to the nucleation of a void in the surface element analyzed (0.5x0.5 mm^2) when ε_{peq} reaches ε^{a}_{peq}.Thus, N_o remains constant and equals 4 voids/mm^2. For each alloy studied, E and F have been identified and are reported in table 4. In the specific case of the TA6Vg alloy,

Table 4: Values of E and F: parameters used for the nucleation kinetics of three different alloys.

	E	F
TA6Va	1.11	4.21
TA6Vg-α/β	4.12	1.96
TA6Vg-α	1.21	2.39
6246	1.28	2.26

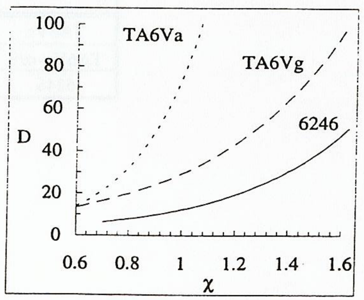

Fig. 5: D *vs* χ for the three alloys. D is associated to α/β voids only.

$N_a = N^{\alpha}_a + N^{\alpha/\beta}_a$ where N^{α}_a and $N^{\alpha/\beta}_a$ are both described by equation 3. An example of the good agreement between equation 3 and experimental results is shown in Fig. 4 for the TA6Va alloy. The comparison of the rate of nucleated voids, D, *versus* triaxiality for the different alloys is shown in Fig. 5. Whatever the stress triaxiality, D increases with the back stress X_s (see table 2). The plastic strain incompatibilities associated to α/β interfaces assist the nucleation kinetics.

Void growth kinetics:

Void growth at the earlier stage of plastic strain produces spherical voids independent of the nucleation location (α or α/β interface). As strain increases, the longest voids are most often elliptic in shape. Assuming that voids width, e, stays constant (2 µm) during void growth, this latter will be characterized in the following by the change in the void length, L. From scanning observations, it appears that void growth begins in the α-particles and then carries on in the β-phase with difficulties (Fig. 6 a, b). This second stage of growth can be assisted by the fracture of the α_s-particles in the vicinity of the principal void. It is well established that void growth rate increases when the yield stress and the hardening rate decrease (Gilormini *et al.*, 1988). This explains why the void growth firstly occurs in the α-phase where the yield stress and the hardening rate are lower than in the β-phase. An experimental analysis of the specimens leads to the plot of the longest void length, L, *versus* triaxiality for given plastic strains or to the plot of L *versus* plastic strain for fixed triaxialities. These two curves are determined for each alloy and show exponential increases (Fig. 7). Such a result has been previously observed in aliminum alloys (Walsh *et al.*, 1989) and in titanium alloys (Narendrnath and Margolin, 1988).

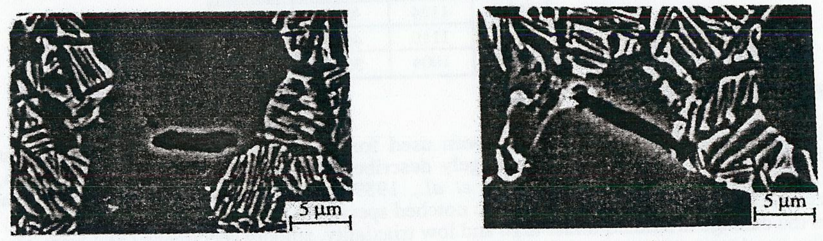

a) b)

Fig. 6: Micrographs of void growth in the α-grains a). Void growth seems to be slowed down by the β-phase b).

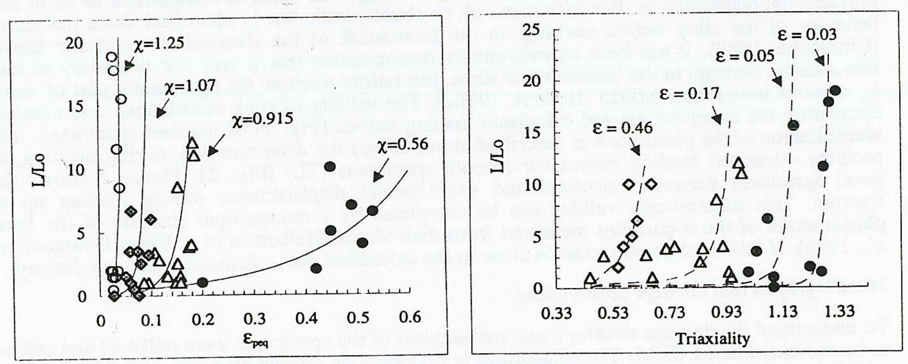

a) b)

Fig. 7: Increase of the longest void length L with plastic strain a), with triaxiality b). (TA6Va)

Numerous studies have provided analytical laws to describe a single-void growth. Various void geometries (cylindrical, spherical) and matrix behaviors (rigid-plastic, linearly or power-law viscous) have been used (Gilormini *et al.*, 1988). These approaches agree with the following classical growth law:

$$dR/R=f(\chi)\, d\varepsilon_{peq} \qquad (4)$$

where R is the mean void radius. In the present work, L will be used instead of R since it characterizes void growth. The void volume equivalence between an ellipsoidal and a spherical void allows the use of an isotropic Gurson model. Among these analyses, the Gurson-Tvergaard model, where the second order terms are neglected, seems to be more appropriate to describe void growth in the α/β titanium alloys since it takes into account a randomly distributed volume fraction f of voids. Gurson's yield function is written as follows:

$$\phi = \Sigma^2_{eq} - \sigma^2_o[1- 2\, q_1\, f \cosh(\tfrac{3}{2}\, q_2\, \chi)] \qquad (5)$$

where q_1 and q_2 were introduced by Tvergaard (Tvergaard, 1981) to bring predictions of the model into closer agreement with full numerical analyses of a periodic array of cylindrical voids. Assuming macroscopic normality, the hydrostatic strain rate, $d\varepsilon_{kk}$, is expressed as:

$$d\varepsilon_{kk} = \tfrac{3}{2}\, f\, q \sinh(\tfrac{3}{2}\, q_2\, \chi)\, d\varepsilon_{peq} \qquad \forall k \in \{1,2,3\} \qquad (6)$$

with $q = q_1 q_2$. Besides, taking into account the plastic incompressibility of the matrix and the mass balance, the void growth law can be written as:

$$df_G = (1-f)\, d\varepsilon_{kk} = (1-f)\, \tfrac{3}{2}\, f\, q \sinh(\tfrac{3}{2}\, q_2\, \chi)\, d\varepsilon_{peq} \qquad (7)$$

From $d\varepsilon_{kk} = f\, dV_{cav}/V_{cav}$ and equation 7, dL/L can be easily deduced assuming that $dV_{cav}/V_{cav} = 3$ dL/L since the void width, e, is a linear function of L. Then, it comes:

$$dL/L = \tfrac{1}{2}\, q \sinh(\tfrac{3}{2}\, q_2\, \chi)\, d\varepsilon_{peq} \qquad (8)$$

From experimental results on void growth kinetics, the constants q and q_2 have been determined for each material (see table 5). q_2 is different from an alloy to the other since, in this first approach, the hardening nature has not been clearly expressed in eq.5. More recently, Mear and Hutchinson (1985) proposed to introduce the effect of the isotropic and kinematic hardening of the matrix in the Gurson's yield function. As it can be seen in table 2, the values of the internal stresses developed in the α/β titanium alloys are quite high. In order to give a better description of the local void growth process, it seems then .necessary to take into account these internal stresses and to define the local triaxiality rate, χ_{loc}, which is involved in void growth. In α-grains, the local triaxiality is written as: $\chi_{loc} = \sigma_m/\sigma_{ef}$ where σ_m is the hydrostatic pressure and σ_{ef} is the effective stress without damage, $\sigma_{ef} = \sigma - X$. Then, $\chi_{loc} = \chi(1+ X/\sigma_{ef})$.

Table 5: Growth parameters: q, q_2 and $\overline{q_2}$.

	q	q2	$\overline{q2}$	(1+Xs/σefs)
TA6Va	1.2	3.5	1.4	2.498
TA6Vg	0.3	3.3	1.4	2.377
6246	0.099	3.6	1.4	2.567

The flow rule is then written as: $\phi = J_2^2(\underline{\underline{\Sigma}}-\underline{\underline{X}}) - \sigma^2_{ef}\,[1-2\, \overline{q_1}\, f \cosh(\tfrac{3}{2}\, \overline{q_2}\, \chi_{loc})]$ (9)

and the growth law form is: $dL/L = \tfrac{1}{2}\, q \sinh(\tfrac{3}{2}\, \overline{q_2}\, \chi_{loc})\, d\varepsilon_{peq}$ (10)

where $J_2(\underline{\underline{\Sigma}}-\underline{\underline{X}}) = [\tfrac{3}{2}(\underline{\underline{S}}-\underline{\underline{X}}):(\underline{\underline{S}}-\underline{\underline{X}})]^{1/2}$ ($\underline{\underline{S}}$ is the deviatoric part of the macroscopic stress $\underline{\underline{\Sigma}}$) and $\underline{\underline{X}}$ is deviatoric. For the alloys studied, the hardening is saturated when damage appears. So, χ_{loc} can be expressed as: $\chi_{loc} = \chi(1+ X_s/\sigma_{efs})$. Comparing eq. 8 and 10, it comes:

$$\overline{q_2}\,(1+ X_s/\sigma_{efs}) = q_2 \qquad (11)$$

From the present calculations, it is found that $\overline{q_2}=1.4$ and remains constant for the alloys studied. This value is in agreement with results on the Ti40 alloy where the internal stresses are low (Huez *et al.*, 1995). $\overline{q_2}$ is associated to void growth in the α-phase. As shown in Fig. 8,

the void growth in the α-phase increases with the internal stresses. Previous studies report that q increases with the initial volume fraction of porosity in the material (Gilormini *et al.*, 1988). In particular, for alloys containing hard inclusions, q has been directly linked to the amount of inclusions (Marini *et al.*, 1985). This dependence on the volume fraction of porosity is often explained as the consequence of interactions between voids which increase the growth rate (Zhang and Niemi, 1995). In the present study, the effect of α-phase percentage on q has not been clearly evidenced, on the contrary, q decreases with increasing λ/ϕ ratio (center-to-center α-particle spacing over the α-particle diameter) (Fig. 9).

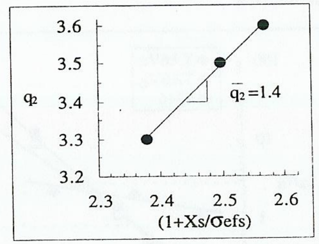

Fig. 8: Change in q_2 as a function of (1+Xs/σefs).

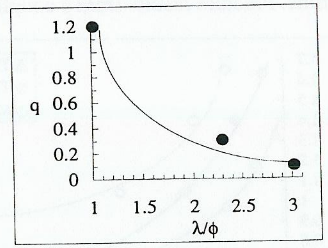

Fig. 9: Change in q as a function of the λ/ϕ ratio.

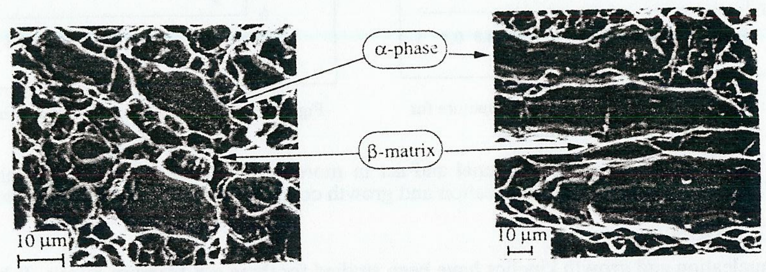

a) b)

Fig. 10: Scanning micrographs of fracture surfaces: a) TA6Vg, b) TA6Va.

As mentioned above, void growth first occurs in the α-grains. Then, the propagation of damage from an α-grain to the other is quite dependent on the microstructure, especially on the λ/ϕ ratio. Indeed, the interactions between voids are higher and the local necking is easier when voids are closer. If a/L is the ratio of the center-to-center α-void spacing out of the α-void length, it has been demonstrated that the constraint factor, σ_n/σ_o (where σ_n is the mean stress in the intervoid matrix), increases when a/L decreases (Thomason, 1985). Then, during loading, the fracture criterion of the matrix is reached first for small a/L ratios. In α/β titanium alloys, the λ/ϕ ratio corresponds to the lowest a/L ratio and is at the origin of the first stage of α-voids coalescence. Besides, according to the alloy, this stage of matrix fracture depends on the nature of the β-phase. On the fracture surface of TA6Vg, a dimple ductile rupture process is observed between two α-voids (Fig. 10a). The fracture is due to the presence of α_s-inclusions in the β-matrix. On the contrary, for the TA6Va, where no inclusions are observed in the β-matrix, the α-void coalescence results from a plastic failure of the β-phase (Fig. 10b).

Fracture process:

The mechanical conditions of fracture, in the space (χ^r, ε^r_{peq}), obtained for different specimens (AE, TL) of each alloy are reported in Fig. 11. Using the nucleation and growth kinetics laws identified above, the volume fraction of voids associated to the nucleation of new voids, f_N (df_N=G dNa, with G=3.14 10^{-6} a geometrical parameter), and the one associated with the growth of actual voids, f_G, have been calculated at fracture for the three alloys. The f_G/f_N ratio at fracture is reported as a function of triaxiality for the three alloys (Fig. 12). For the TA6Vg and the 6246 alloys, three domains must be distinguished with the triaxiality:

- Under low stress triaxiality, $f_G/f_N < 1$. The growth process is negligible and the nucleation kinetics is the cause of fracture.
- For high triaxialities, $f_G/f_N > 1$. The nucleation process can be neglected in front of the growth process which involves fracture.
- In a middle range of triaxialities, the nucleation and growth processes occurs at the same time. Fracture results from a coupling of the two processes.

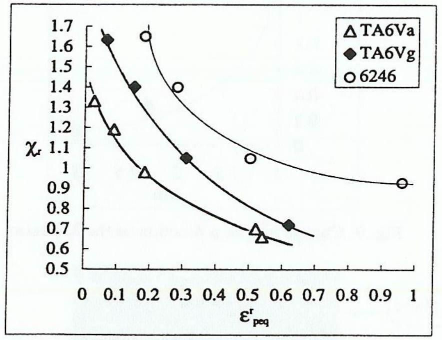

Fig. 11: Mechanical couples (χ^r,ε^r_{peq}) at fracture for the specimens of each material.

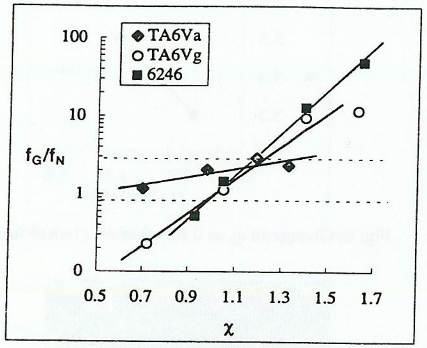

Fig. 12: f_G/f_N ratio as a function of triaxiality for the three alloys.

These domains depend on the material and act in more or less large range of triaxiality. The TA6Va, for example, presents nucleation and growth coupling in a large range of triaxiality.

CONCLUSION

Void nucleation and growth kinetics have been studied for three α/β titanium alloys. It has been evidenced that the internal stresses increase both nucleation and growth rates. The first growth stage occurs in α-grains, and the second stage is mainly dependent on the β-matrix fracture process. The growth rate of this second stage increases when the microstructural λ/ϕ ratio decreases. Three fracture modes have been identified depending on triaxiality and on the alloy. Under low triaxiality, fracture occurs by a nucleation process. Under high triaxiality, void growth and coalescence process lead to fracture. Finally, in the middle range of triaxiality, both nucleation and growth processes occur at the same time.

REFERENCES

Argon A.S. and Im J. (1978). Separation of inclusions in spheroidized 1045 steel, Cu-0.6% Cr alloy, and Maraging steel in plastic straining. *Met. Trans.*, 6A, 839.

Becker R., Needleman A., Richmond O. and Tvergaard V. (1988). Void growth and failure in notched bars. *J. Mech. Phys. Solids*, 36, 317-351.

Beremin F.M. (1981). Cavity formation from inclusions in ductile fracture of A508 stell. *Met. Trans.*, 12A, 723-731.

Bourgeois M., Feaugas X. and Clavel M. (1996). Fracture of an α/β titanium alloy under stress triaxiality states at 773 K. *Scripta Met.*, 34, 1483-1490.

Brownrigg A., Spitzig W.A., Richmond O., Tierlinck D. and Embury J.D. (1983). The influence of hydrostatic pressure on the flow stress and ductility of the spheroidized 1045 steel. *Acta Met.*, 31, 1141-1150.

Chu C.C. and Needelman A. (1980). Void nucleation effects in biaxialy stretched sheets. *J. of Eng. Mat. and Tech.*, 102, 249-256.

Feaugas X., Pilvin P. and Clavel M. (1995). Modélisation micromécanique du comportement d'un alliage de titane biphasé α/β. *Proceedings on the Zirconium 95 conference*, INSTN Saclay, France.

Gilormini P., Licht C. and Suquet P. (1988). Growth of voids in ductile matrix: a review. *Arch. Mech.*, 40, 43-80.

Greenfield M.A. and Margolin H. (1972). The mechanisms of void formation, void growth, and tensile fracture in an alloy consisting of two ductile phases. *Met. Trans.*, 3A, 2649-2659.

Hancock J.W. and Brown D.K. (1983). On the role of strain and stress state in ductile failure. *J. Mech. Phys. Solids*, 31, 1-24.

Helbert A.L., Feaugas X. and Clavel M. (1996a). The influence of stress triaxiality on the damage mechanisms in an equiaxed α/β Ti-6Al-4V alloy, *Met. Trans.*, to be published.

Helbert A.L., Feaugas X. and Clavel M. (1996b). Cartes d'endommagement d'alliages de titane. *La revue de Metallurgie*, to be published.

Helbert A.L., Feaugas X. and Clavel M. (1996c). The influence of the back stress (X) and the hardening rate ($dX/d\varepsilon_{peq}$) on void nucleation in α/β titanium alloys. *Jounal de physique. Proceedings on the first European Mechanics of Materials Conference. MECAMAT'96.*

Huez J., Feaugas X. (1995). Damage process in Ti40 and Ti40-H. private comunication.

Le Roy G., Embury J.D., Edwards G. and Ashby M.F. (1981). A model of ductile fracture based on the nucleation and growth of voids. *Acta Met.*, 29, 1509-1522.

Margolin H., Williams J.C., Chesnutt J.C. and Lüetjering G. (1980). A review of the fracture and fatigue behavior of Ti alloys. *Titanium '80, Science and technology*, 1, 169-216.

Marini B., Mudry F. and Pineau A. (1985). Experimental study of cavity growth in ductile rupture. *Eng. Frac. Mech.* , 22, 989-996.

Mear M.E. and Hutchinson J.W. (1985). Influence of yield surface curvature on flow localization in dilitant plasticity. Mech. of Mat., 4, 395-407.

Narendmath K.R. and Margolin H. (1988). The effect of matrix strength on void nucleation and growth in a widmanstätten alpha-beta titanium alloy, CORONA-5., *Met. Trans.*, 19A, 1163-1171.

Thomason P.F. (1985). Three-dimensional models for the plastic limit-loads at incipient failure of the intervoid matrix in ductile porous solids. *Acta Metall.*, 33, 1079-1085.

Tvergaard V. (1981). Influence of voids on shear band instabilities under plain strain conditions. *Int. J. of Fract.*, 17, 389-407.

Walsh J.A., Jata K.V. and Starke E.A. jr (1989). The influence of Mn dispersoide content and stress state on ductile fracture of 2134 type Al alloys. *Acta Met.*, 37, 2861-2871.

Zhang Z.L. and Niemi E., (1995). A new criterion for Gurson-Tvergaard dilational constitutive model. *Int. J. of Fract.*, 70, 321-334.